Biomass Conversion and Biorefinery (2021) 11:1875–1883
https://doi.org/10.1007/s13399-019-00591-2

ORIGINAL ARTICLE

Comparison study on potential syngas produced by mild thermoconversion of microalgal residues through proton nuclear magnetic resonance and thermogravimetric analysis-fourier transform infrared spectroscopy

Shuangfei Li[1] · Liangxu Liu[1] · Jay Jiayang Cheng[2] · Xuewei Yang[1]

Received: 10 September 2019 / Revised: 22 December 2019 / Accepted: 26 December 2019 / Published online: 16 January 2020

Abstract
This paper presented a mechanism study of syngas production through lipid-extracted microalgal residues by investigating how the structure of these residues affected the pyrolysis characteristics. The results showed that both *Chlorella sorokiniana* 21 and *Monoraphidium* 3s35 residues could be pyrolyzed efficiently at low temperatures from 120 to 380 °C, with a final residue of less than 22.75%. Hemicellulose with carboxyl groups was the main component of both microalgal residues, most likely contributing to the production of the C=O compounds and carbon monoxide (CO). A large amount of CHO, CH_2O, and CH_3O (60.09% in total) was observed from *C. sorokiniana* 21, which was 1.58 times more than that from *Monoraphidium* 3s35. Pyrolysis of the *C. sorokiniana* 21 residue yielded more C=O and CH_n compounds with less activation energy (52.97–58.57 kJ mol^{-1}) and a higher reaction rate (0.105% s^{-1}) than that of *Monoraphidium* 3s35. The different pyrolysis characteristics between the two microalgal residues might be attributed to structural variations.

Keywords Microalgal residue · Structure · Pyrolysis · Thermogravimetric characteristics

1 Introduction

Biomass has been considered one of the most promising renewable energy sources in the world. Compared with fossil fuels, biomass can be processed into liquid transportation fuels, which can substantially decrease the net emissions of carbon into the atmosphere [1]. Biomass can be obtained from land crops as well as ocean habitats. Microalgae, known as sunlight-driven cell factories, can convert carbon dioxide to potential biofuel materials [2] and are an important source of biomass, with the merits of high yields and a short life cycle [3].

✉ Xuewei Yang
yangxw@szu.edu.cn

[1] Shenzhen Key Laboratory of Marine Biological Resources and Ecology Environment, Shenzhen Key Laboratory of Microbial Genetic Engineering, College of Life Sciences and Oceanography, Shenzhen University, Shenzhen 518055, People's Republic of China

[2] Department of Biological and Agricultural Engineering, North Carolina State University, Raleigh, NC 27695, USA

There have been major challenges in biochemically converting lignocellulosic biomass into biofuel due to the complex structure of the biomass and the difficulty of separating its components in an economically feasible way [4]. Pyrolysis, however, has provided an alternative solution for converting cellulosic biomass into renewable energy and valuable chemicals [5]. In the last decade, intensive pyrolysis research has been performed on lignocellulosic biomass, ranging from agricultural residues such as corn stover and wheat straw to energy crops such as switchgrass [6]. Forestry wastes such as wood bark have also been the targets for pyrolysis [5]. Research on microalgal biomass pyrolysis using Py-GC/MS and DAEM [7] has been reported. Thermal degradation of the microalgae *Chlorella vulgaris* ESP-31, *Nannochloropsis oceanica* CY2, and *Chlamydomonas* sp. JSC4 has also been analyzed [8]. Recently, microalgae have mainly been used for lipid and biodiesel production [9]. The reutilization of residues after the biofuel conversion process is significant for increasing the economic efficiency of microalgae. However, the mechanism of pyrolysis for lipid-extracted microalgal residues has barely been reported. The online combination of thermogravimetric analysis (TGA) and fourier transform

infrared (FTIR) spectroscopy has been successfully applied to the study of the evolution of volatile products with time in the thermal pyrolysis of polymers [10] as well as *Nannochloropsis* sp. [11]. It is important to understand the mechanism of microalgal residue pyrolysis, the thermogravimetric decomposition of the volatile products, and the influence of the composition and structure of the microalgae on the pyrolysis kinetics.

In this study, lipid-extracted residues of the microalgae *Chlorella sorokiniana* and *Monoraphidium* were investigated with TGA/FTIR to elucidate their dynamic pyrolysis behavior including kinetics and volatile products produced. Furthermore, the chemical structures of the two microalgal residues were analyzed with proton nuclear magnetic resonance (^{1}H NMR) spectroscopy to determine the influence of the structural variation on the pyrolysis.

2 Materials and methods

2.1 Microalgal residue preparation

The microalgal strains *Chlorella sorokiniana* 21 and *Monoraphidium* 3s35 used in this study were collected from the coastal waters of Shenzhen, Guangdong Province, China. Blue-green medium (BG-11) with 1.5% agar supplement was used to maintain the strains [12]. Each individual cultivation test was carried out with 3 replicates for 10 days. Slots on an incubation shaker platform (Constant Temperature Breeding Shaker, MOMA, Shanghai, China) were randomly assigned. To initiate the cultivation, 80 mL of axenic culture in the exponential phase (dry cell mass density 50 ± 0.08 mg L^{-1}) was inoculated into 1 L flasks with 800 mL of sterile BG-11 medium. The flasks were covered with autoclavable foam and cultivated at a room temperature of 26 °C with an initial pH of 7.1. Three rows of cool white portable fluorescent light tubes (PM-RGT8-30 W, Mei Optoelectronics Technology Company, Foshan, Guangdong Province, China) were used with a light intensity of 100.5 μmol m^{-2} s^{-1} ±2.0 SE. Aeration of 0.25–0.75 L air per minute was applied to each cultivation flask. To collect the microalgal biomass, the cultures were centrifuged (Centrifuge 5810R, Eppendorf, Germany) at 4000×*g* for 20 min and resuspended in distilled water. After repeating the above process 3 times, the microalgal biomass was freeze-dried (FreeZone 2.5, LABCONCO, USA) for 3 days. A Soxhlet extractor was used for lipid extraction from the previously obtained microalgal biomass, with 1.5 g extracted with chloroform/methanol (1/2, v/v) at 75 °C for 12 h. After lipid extraction, the microalgal residues were then dried at 30 °C under vacuum for 12 h. Three biological replicates for each sample of the microalgae biomass residue were prepared for further experiments.

2.2 Microalgal residue composition analysis

Microalgal residue composition analysis was performed through the method of the Association of Official Analytical Chemists (AOAC) (1984) [13], which has also been used for analyzing the composition of marine algae *Enteromorpha* spp. [14], *Schizochytrium* sp. [15], *Spirulina* algae [16], and the microalga *Porphyridium cruentum* [17]. Dried algal samples were analyzed for neutral detergent fiber (NDF) [18], acid detergent fiber (ADF) [19], acid detergent lignin (ADL) [20], and ash in ADL according to the procedures of Van Soest et al. (1991) and AOAC (1984) [13]. Hemicellulose, cellulose, and Klason lignin contents were determined by the differences between ADF and NDF content, ADF and ADL content, and ADL and ash content, respectively [21]. Three biological and measurement replicates were performed throughout this study.

2.3 Algal biomass structure analysis with ^{1}H NMR spectroscopy

^{1}H NMR spectra of microalgal residues were obtained by a Bruker 500 Ultrashield I100605 400-MHz spectrometer outfitted with a 5-mm broadband probe (Borosilicate Glass Company, China). Firstly, 20 mg of microalgal residue was dissolved in 1 mL of DMSO-d_6 (dimethyl sulfoxide-d6), filtered with a 0.45-μm PTFE (poly tetra fluoroethylene) filter to remove any suspended particulates, and then loaded into 5-mm diameter NMR tubes [22]. Three measurement replicates were performed throughout this study.

2.4 Thermogravimetric analysis with TG-FTIR (thermogravimetric analysis coupled with fourier transform infrared analysis)

The thermogravimetric characteristics of the microalgal residues were determined by thermogravimetry coupled with Fourier transform infrared (TG-FTIR) analysis (STA449 F3, Naichi Instrument Company, China; TENSOR27 FTIR, Bruker, Germany). High-purity N_2 was used as the protective gas at a flow rate of 20 cm^3 min^{-1}. Approximately 10 mg of microalgal residue was heated from 25 to 650 °C at 10 °C min^{-1} and then held for 1 h at the highest temperature. The volatiles released during pyrolysis of the microalgae were detected online with a Bruker FTIR Tensor Spectrometer (TENSOR27 FTIR, Bruker, Germany). FTIR spectra were recorded from 400 to 4000 cm^{-1}. Before the microalgal samples were processed in the system, a blank test was carried out first to eliminate the buoyancy effect. Three measurement replicates were performed throughout this study.

2.5 Microalgae pyrolysis kinetics

The Arrhenius equation used in previously reported work was employed to describe the pyrolysis reaction rate in this study as follows [7]:

$$\frac{dX}{dt} = -Ae^{-\left(\frac{E}{RT}\right)}X^n \quad (1)$$

where the notation of the Arrhenius equation X (Eq. (1)) was defined as the extent of the pyrolysis reaction. The conversion value X was determined as $(w\text{-}w_f)/(w_0\text{-}w_f)$, t is the time of reaction, A is the pre-exponential or frequency factor, E is the activation energy, R is the universal gas constant, T is the absolute temperature, and n is the order of reaction. The linearized form of the Arrhenius equation was used to determine the kinetic constants A, E, and n. The simplified form of the linearized Arrhenius equation is as follows:

$$1n\left(\frac{-1}{w_0-w_f}\frac{dw}{dt}\right) = 1nA-\left(\frac{E}{RT}\right) + n1n\left(\frac{w-w_f}{w_0-w_f}\right) \quad (2)$$

where w_0 is the initial weight at the beginning of the pyrolysis, w_f is the final weight at the end of each stage of the pyrolysis (details are explained in a later section), and w is the weight at any time of the pyrolysis process.

Eq. (2) can be written in linear form [7]:

$$y = B + Cx + Dz \quad (3)$$

where y, x, z, B, C, and D (Eq. (3)) are defined as follows (Eqs. (4)–(6)):

$$y = 1n\left(\frac{-1}{w_0-w_f}\frac{dw}{dt}\right) \quad (4)$$

$$x = \frac{1}{RT} \quad (5)$$

$$z = 1n\left(\frac{w-w_f}{w_0-w_f}\right) \quad (6)$$

$$B = 1nA \quad (7)$$

$$C = -\frac{E}{R} \quad (8)$$

$$D = n \quad (9)$$

The constants B, C, and D were estimated with multilinear regression of the TGA data for each stage using Microsoft Excel (Microsoft, Seattle, USA). The kinetic parameters (A, E, and n) were determined according to Eqs. (7), (8), and (9). Three measurement replicates were performed throughout this study.

The data were analyzed with Statistical Package of the Social Sciences (SPSS) software (Windows version 7.0, SPSS, Inc., Chicago, IL). Paired t test was used to analyze continuous data. A p value < 0.05 was considered significant.

3 Results and discussion

3.1 Chemical composition and structure of *C. sorokiniana* 21 and *Monoraphidium* 3s35 residues

The chemical compositions of the microalgal residues of *C. sorokiniana* 21 and *Monoraphidium* 3s35 are presented in Table 1. As shown in the table, hemicellulose was the major component (over 40% dry-weight basis) of both microalgal residues. This finding is consistent with the chemical composition research on the marine algae *Enteromorpha* spp., in which the dominant component of the cellular wall is hemicellulose [23]. Cellulose and lignin were observed as the minor components in both microalgae (less than 3%). Previous research has reported that the polysaccharides of sea algae can be divided into cell wall polysaccharides such as cellulose and hemicellulose [24]. Lignin-like compounds and lignin were also discovered in the cell wall of the red alga *Calliarthron cheilosporioides* and *Coleochaete* algae [25]. Statistical analysis indicated that there was no significant difference in the composition between the two microalgal residues [26].

To assess differences in the chemical structure of *C. sorokiniana* 21 and *Monoraphidium* 3s35, we acquired ^{1}H NMR spectra to compare the functional group differences, as shown in Fig. 1 and Table 2. Both microalgal residues contained more than 13% alkanes based on the integrated peaks of CH_3 and CH_2 (0–1.6 ppm). Notably, *C. sorokiniana* 21 contains a large amount of CHO, CH_2O, and CH_3O (60.09% in total), which is 1.58 times more than that in *Monoraphidium* 3s35 (only 38.12%). In addition, the functional groups of ArOH, HC=C (nonconjugated), and CHO accounted for 31.51% in *Monoraphidium* 3s35, which is 4.81 times more than that in *C. sorokiniana* 21 (6.55%).

Overall, although there is no significant difference between the compositions of these two microalgae, structural variation was observed: *C. sorokiniana* 21 contained more CHO,

Table 1 Chemical composition of microalgl residue *Chlorella sorokiniana* 21 and *Monoraphidium* 3s35. Data are shown as mean ± standard deviation ($n = 3$)

Composition (% dry based)	Sample	
	Monoraphidium 3s35	*C. sorokiniana* 21
NDF[a]	45.98 ± 0.79	47.11 ± 1.74
ADF[b]	4.43 ± 0.35	4.73 ± 0.44
Cellulose	2.82 ± 0.11	2.70 ± 0.59
Hemicellulose	41.56 ± 1.13	42.38 ± 2.12
Lignin	2.42 ± 0.04	2.64 ± 0.53

[a] *NDF*:neutral detergent fiber

[b] *ADF* acid detergent fiber

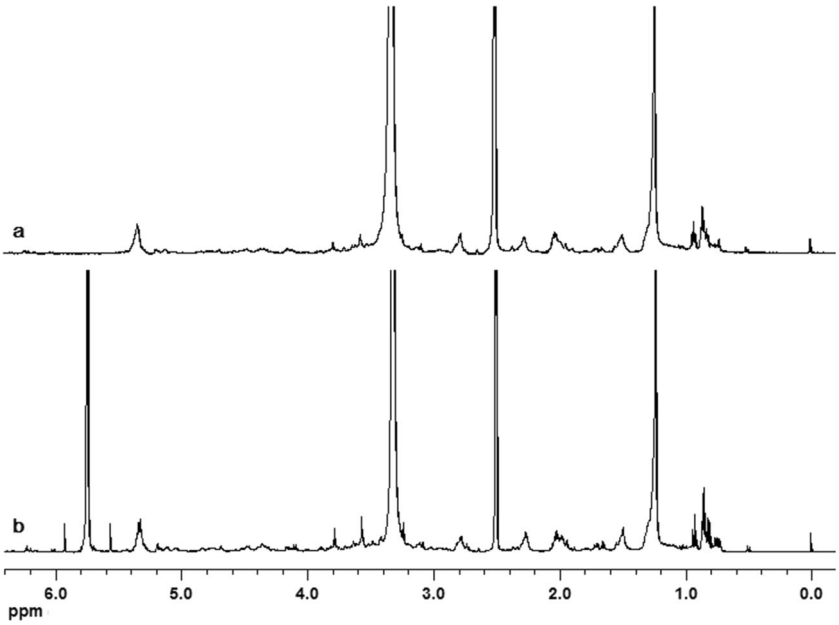

Fig. 1 Proton nuclear magnetic resonance (^{1}H NMR) spectra of microalgal residue. **a** *Chlorella sorokiniana* 21. **b** *Monoraphidium* 3s35

CH_2O, and CH_3O groups, and *Monoraphidium* 3s35 contained more ArOH and HC=C groups. It was reported that there are two different kinds of structures in cellulose: crystalline and amorphous domains. Depending on both source and history, cellulose consists of these crystalline and amorphous domains in varying proportions [27]. The presence of amorphous cellulose was indicated by strong C-H stretching vibrations, and the C-O-C stretching vibrations attributed to α-(1-4)-glycosidic linkages were designated as an "amorphous" absorption band, indicating an intensity increase in the amorphous cellulose. The different chemical compositions of cellulose could lead to various thermal decomposition results.

3.2 Pyrolysis of *C. sorokiniana* 21 and *Monoraphidium* 3s35 residues

3.2.1 Thermogravimetric characteristics

Thermogravimetric analysis Figure 2 shows the thermogravimetry (TG) and derivative thermogravimetry (DTG) results of the microalgal residues of *C. sorokiniana* 21 and *Monoraphidium* 3s35 in the pyrolysis process. Both microalgal residues had three distinct weight loss stages during thermal degradation: dehydration, active pyrolysis, and passive pyrolysis, with temperature ranges of 25–120 °C, 120–500 °C, and 500–650 °C, respectively. The active pyrolysis stage contained two substages, which was different from the pyrolysis of plant lignocellulosic biomass such as corn stover [28]. The active pyrolysis temperature for hemicelluloses is usually from 190 to 360 °C, so the appearance of active pyrolysis substage 1 (120 to 380 °C) is likely attributed to the large amount of hemicelluloses in the microalgal residue. The TG results also revealed that the final residue yields of the microalgal residue (22.20% for *C. sorokiniana* 21 and 22.75% for *Monoraphidium* 3s35) were significantly lower than those of plant lignocellulosic biomass, such as corn stover (33.32%) [29] and rice straw (29.5%) [30]. This result indicated that the thermal decomposition of microalgal residue can be more efficient than that of lignocellulosic biomass.

Table 2 ^{1}H NMR (proton nuclear magnetic resonance) spectral distribution analysis of functional groups present in the microalgal residues based on integrated peak areas assigned to characteristic spectral regions and chemical shift range. Data are shown as mean±standard deviation ($n = 3$)

Assignments	Chemical shifts (ppm)	*C. sorokiniana* 21 (%)	*Monoraphidium* 3s35 (%)
CH_3, CH_2	0–1.6	13.99 ± 0.23	16.47 ± 0.49
CH_2, aliphatic OH	1.6–2.2	2.51 ± 0.31	3.43 ± 0.45
CH_2C=O, CH_3-Ar, -CH_2-Ar	2.2–3	14.56 ± 0.17	10.01 ± 0.53
CH_3O, CH_2O, CHO	3–4.2	60.09 ± 0.51	38.12 ± 0.22
ArOH, HC=C (non-conjugated), CHO	4.2–6.4	6.55 ± 0.42	31.51 ± 1.02
HC=C (non-conjugated)	6.4–6.8	0.63 ± 0.12	0.11 ± 0.08
ArH, HC=C (conjugated)	6.8–8	1.00 ± 0.11	0.09 ± 0.06
CHO, COOH	8–10	0.07 ± 0.02	0.25 ± 0.09

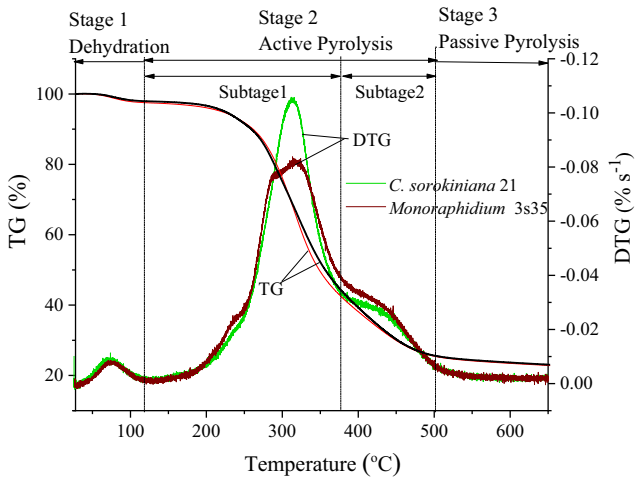

Fig. 2 Thermogravimetry (TG)/derivative thermogravimetry (DTG) diagrams of microalgae *Chlorella sorokiniana* 21 and *Monoraphidium* 3s35 residues in a pure nitrogen environment

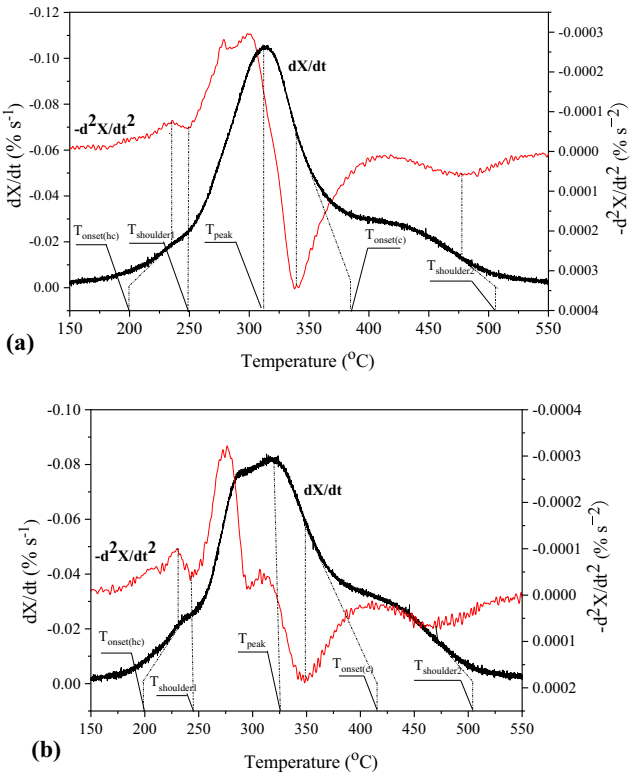

Fig. 3 The first and the second time derivatives of the mass fraction as functions of temperature for the microalgal residues and definitions of the characteristic reaction temperatures. **a** *Chlorella sorokiniana* 21. **b** *Monoraphidium* 3s35

As shown in Fig. 2, the DTG curve for each microalgal residue had two peaks for the reaction rate (−dX/dt) of the pyrolysis. It was also observed that the reaction rate of microalgae pyrolysis increased rapidly from 115 to 310 °C and then dropped dramatically from 310 to 504 °C with a shoulder from 384 to 445 °C. In substage 1, the peak of the reaction rate for *C. sorokiniana* 21 (0.105% s^{-1}) was much higher than that for *Monoraphidium* 3s35 (0.0799% s^{-1}).

d^2X/dt^2 analysis of TG According to Grønli et al. [31], temperatures for the thermal degradation of hemicellulose, cellulose, and lignin could be defined with d^2X/d^2t analysis. The d^2X/d^2t temperature curves obtained in this study are shown in Fig. 3. As shown in the figure, the characteristics of the thermal decomposition of the microalgal residue can be quantified through the following parameters:

$T_{onset(hc)}$ is the extrapolated temperature at the beginning of hemicellulose decomposition;

$T_{shoulder1}$ is the temperature corresponding to the hemicellulose shoulder;

T_{peak} is the temperature of the maximum devolatilization rate during the entire pyrolysis;

$T_{onset\ (c)}$ is the extrapolated temperature for the cellulose decomposition;

$T_{shoulder2}$ is the temperature corresponding to the cellulose shoulder and the beginning of the lignin tail in which lignin degradation occurs.

As shown in Fig. 3, the hemicelluloses of the *C. sorokiniana* 21 and *Monoraphidium* 3s35 residues started to be thermally decomposed at a $T_{onset(hc)}$ of 193 °C and 191 °C, respectively and reached the maximum reaction rate at a T_{peak} of 310 °C and 311 °C. There was a pyrolysis shoulder observed for the microalgae *C. sorokiniana* 21 and *Monoraphidium* 3s35 residues at a $T_{shoulder1}$ of 248 °C and 240 °C, respectively. Although the amount of cellulose in microalgal residue is much less than that in lignocellulosic biomass, the structure of cellulose is complicated and crystalline [32], compared with that of hemicelluloses. Thus, the pyrolysis stage of cellulose can be observed in Fig. 3. According to this figure, the cellulose of the microalgae *C. sorokiniana* 21 and *Monoraphidium* 3s35 residues began thermally decomposing at a $T_{onset\ (c)}$ of 390 °C and 408 °C, respectively. It has been reported that the weight loss of cellulose during pyrolysis happens at 315–400 °C [33], which was consistent with our results. The lignin of the microalgae *C. sorokiniana* 21 and *Monoraphidium* 3s35 residues began pyrolysis at a $T_{shoulder2}$ of 512 °C and 504 °C, respectively.

3.2.2 Microalgae pyrolysis kinetics

The kinetic parameters for the microalgae pyrolysis in substages 1 and 2 during the active pyrolysis stage are presented in Table 3. As shown in the table, the activation energy of the microalgae pyrolysis in substage 1 (52.97–58.57 kJ mol^{-1}) was much lower than that in substage 2 (82.50–83.98 kJ mol^{-1}). It was reported that the peaks of the distribution curve of the activation energy for rice straw, rice husk, corncob, and cellulose were 170, 174, 183, and 185 kJ mol^{-1} [34], respectively. It is known that the activation energy represents the potential barrier needed to be overcome in the

Table 3 Kinetic parameters of the microalgae residue active pyrolysis at the heating rate of 10 k min^{-1} in the pure nitrogen environment

Kinetic parameters	Microalgal residues	
	C. sorokiniana 21	*Monoraphidium* 3s35
Substage 1 (120 °C–380 °C)		
A (10^4 s^{-1})	0.95	0.04
E (kJmol^{-1})	52.97	58.57
n	1.46	2.21
R^2	0.95	0.96
Substage 2 (380 °C–500 °C)		
A (10^4 s^{-1})	5.15	5.94
E (kJmol^{-1})	82.50	83.98
n	2.34	2.24
R^2	0.92	0.93

reaction [35]. Compared with lignocellulose biomass, microalgae require less energy to start the thermogravimetric reaction. The results also showed that the activation energy of the residue of *C. sorokiniana* 21 was less than that of *Monoraphidium* 3s35, indicating that the former is more easily pyrolyzed and has a lower energy barrier.

3.2.3 Volatile products analysis of TG-FTIR

To identify the major volatile species and continuously measure the volatiles and the devolatilization temperature during microalgae pyrolysis, TG analysis coupled with FTIR spectroscopy was applied in this study. The TG-FTIR spectra of these two microalgae are shown in Fig. 4. The composition of the volatile products was determined with the characteristic wavenumber bands, while the yield history of the products in the time course was identified by the absorbance against time. An integral form of the Lambert-Beer relation was used for the abovementioned determination and identification [36]. The integrated absorbance (IA, measured in cm^{-1}) is the integral value of the spectral absorbance over a selected wavenumber interval characteristic for the compound of interest, which can give a quantitative measure of the gaseous species detected.

During the pyrolysis of microalgal residues, light gases (namely, C=O compounds, CH_n compounds, CO_2, and CO) were detected in the specific wavenumber intervals listed in Table 4. The results are shown in Fig. 5. Compounds with characteristic carbonyl bonds, typically organic acids, esters, aldehydes, and ketones, are called C=O compounds [37]. Compounds with characteristic C-H bonds, typically alkyl, aliphatic, and aromatic compounds, can be classified as CH_n compounds.

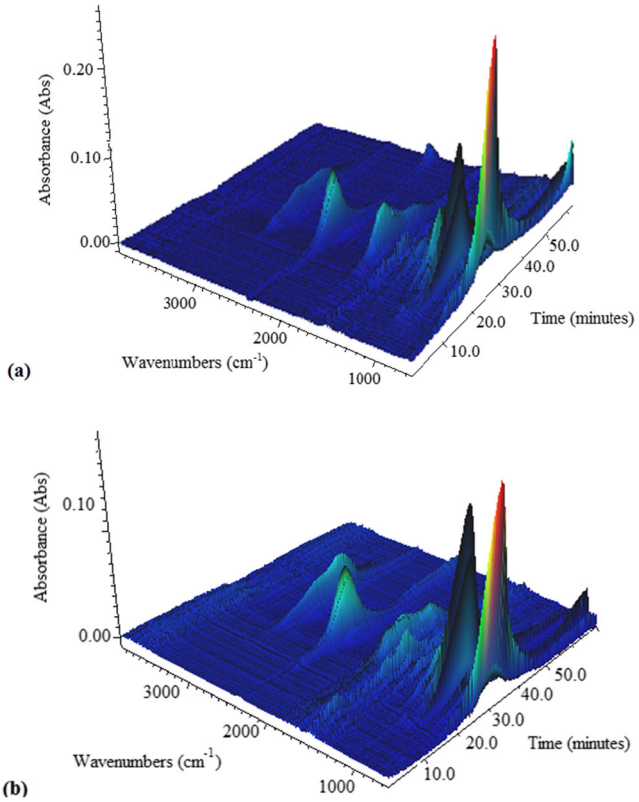

Fig. 4 Three-dimensional spectra of TG–FTIR (thermogravimetric analyzer coupled with fourier transform infrared analysis). **a** *Chlorella sorokiniana* 21. (b) *Monoraphidium* 3s35

C=O compounds As shown in Fig. 5a, two peaks were observed for the production of C=O compounds (R–CHO and R–COOH) during the pyrolysis of both *C. sorokiniana* 21 and *Monoraphidium* 3s35. According to our results, the temperatures for the maximum production of C=O compounds from the pyrolysis of *C. sorokiniana* 21 and *Monoraphidium* 3s35 were 251 °C and 333 °C, respectively. The active pyrolysis temperature for hemicelluloses is usually from 190 to 360 °C. The compositions of hemicellulose in the microalgae *C. sorokiniana* 21 and *Monoraphidium* 3s35 were 41.56% and 42.38%, respectively. The production of the C=O compounds is probably due to the pyrolysis of hemicellulose in the microalgae. It was reported that the pyrolysis of *Chlorella vulgaris* microalgae occurred in the temperature range of

Table 4 Wavenumber intervals of different gaseous species for the definition of the integrated absorbance during the microalgal residue pyrolysis analyzed with TG-FTIR (thermogravimetric analyzer coupled with fourier transform infrared analysis)

Gas species	Wavenumber interval (cm^{-1})
CH_n group	2832–3027
CO_2	2220–2393
CO	2142–2218
C=O group	1835–1673

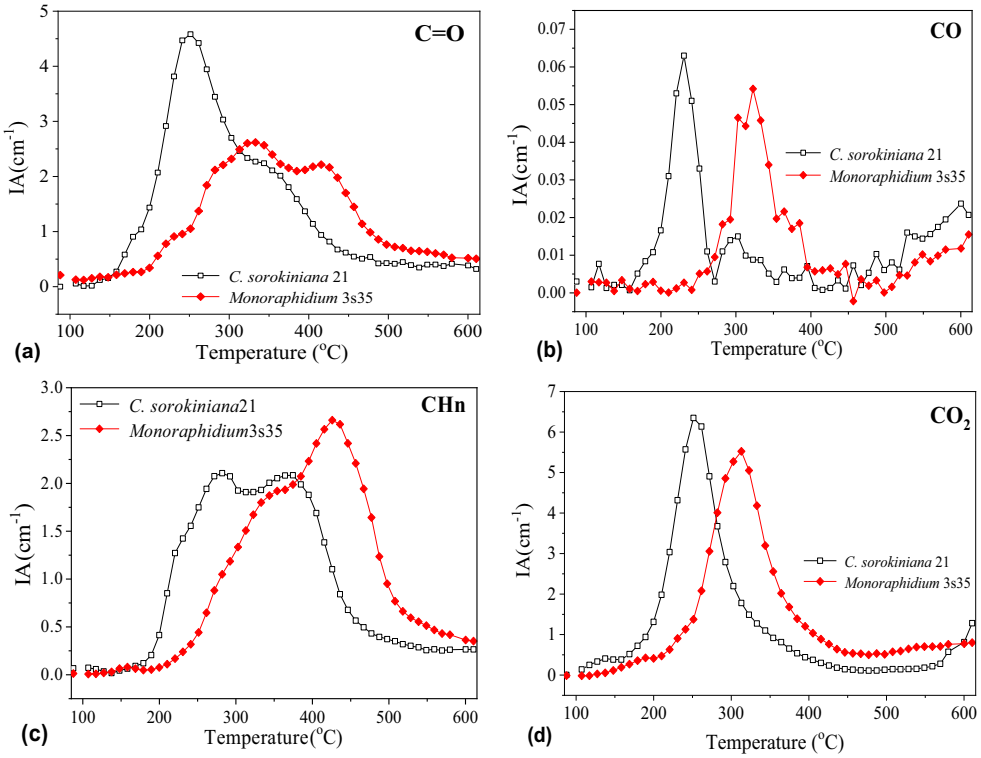

Fig. 5 Fourier transform infrared (FTIR) integrated absorbance profiles of main gaseous species evolved in the pyrolysis of microalgal residue *Chlorella sorokiniana* 21and *Monoraphidium* 3s35

133–537 °C, and the main weight loss peak occurred at approximately 296 °C, which is consistent with our results. At low temperatures, hemicellulose decomposition contributes to C=O and COOH functional group generation [3]. Hemicelluloses are heterogeneous polymers of pentoses (xylose, arabinose), hexoses (mannose, glucose, galactose), and sugar acids, with a random, amorphous structure. The backbone of hemicellulose consists of O-acetyl, α-l-arabinofuranosyl, α-1,2-linked glucuronic, or 4-O-methylglucuronic acid substituents. The release of carbonyl groups can be caused by the cracking of xylan and glucomannan from hemicellulose [4]. Acidic products, especially acetic acid and formic acid, with C=O groups, are commonly detected in the bio-oil from the pyrolysis of hemicellulose [5]. The prevalent mechanism of the formation of acetic acid involves a primary elimination reaction of the active O-acetyl groups linked to the main xylan chain at the C2 position [6].

Carbon monoxide Carbon monoxide (CO) released from pyrolysis of the microalgae is shown in Fig. 5b. The peaks of CO release were observed at 230 °C and 323 °C for *C. sorokiniana* 21 and *Monoraphidium* 3s35, respectively. *C. sorokiniana* 21 reached a higher maximum production of CO at a lower temperature than did *Monoraphidium* 3s35. Since the release of CO was mainly caused by the cracking of ether (C-O-C) and carboxyl (C=O) groups [38], the superiority of *C. sorokiniana* 21 in producing CO might be attributed to the chemical structure difference between these two microalgae. On the other hand, it has been reported that the release of CO from cellulose was very small, with only a small peak, and that almost no CO was evolved from lignin pyrolysis at low temperature (< 600 °C) [33]. The authors also reported that there was a peak for CO release from hemicelluloses at 280 °C, which was within the temperature range for CO release in our observation. Thus, we believe that the CO production of microalgal residues is mainly from hemicelluloses.

CH_n compounds The CH_n compounds released from pyrolysis of the microalgal residues are shown in Fig. 5c. As shown in the figure, the CH_n compounds showed two main release peaks at 278 °C and 378 °C for *C. sorokiniana* 21 and a shoulder from 322 to 385 °C for *Monoraphidium* 3s35. The primary pyrolysis may give rise to the first release peak, while the secondary pyrolysis at a higher temperature might be the driving force for the second release peak of gases, which is in agreement with a report by Yang et al. (2007). The first release peak of CH_n compounds from *C. sorokiniana* 21 might be caused by the cracking of the high content of CH_3O compounds as shown in Table 2. The cracking procedure mainly happened during primary pyrolysis at low temperature. For *Monoraphidium* 3s35, the production of CH_n compounds might be due to secondary pyrolysis. It was reported that 1,4-anhydro-d-xylopyranose is one of the main condensable products from hemicellulose pyrolysis, which is attributed to cleavage of the glycosidic linkage of the xylan chain, followed by rearrangement of the depolymerized molecules. Studies

have inferred that most of the produced 1,4-anhydro-d-xylopyranose would be instantly consumed to produce two-carbon and three-carbon fragments as well as gases including CH_4, acting as an intermediate product from the pyrolysis of hemicellulose [5].

Carbon dioxide Carbon dioxide (CO_2) released from pyrolysis of the microalgae is shown in Fig. 5d. As shown in the figure, CO_2 generation reached a peak at 250 °C and 313 °C for *C. sorokiniana* 21 and *Monoraphidium* 3s35, respectively. Based on the results, *Monoraphidium* 3s35 produced less CO_2 than *C. sorokiniana* 21 during pyrolysis. The production of CO_2 is due to the cracking and scission of C-C and C-O bonds during pyrolysis [39].

4 Conclusion

The present study showed that microalgal residues have clear advantages over plant lignocellulosic materials in terms of pyrolysis, with a lower activation energy (52.97–83.98 kJ mol^{-1}) and lower final residue yields (22.20–22.75%). Due to the high content of hemicellulose (41.56–42.38%) and the predominant structure of carboxyl and carbonyl functional groups, the main evolution products were C=O and CH_n compounds, presenting great potential as syngas. Moreover, the chemical structure differences between *C. sorokiniana* 21 and *Monoraphidium* 3s35 probably resulted in the observed variation in the pyrolysis characteristics and production of volatiles.

Authors' contributions Details of the individual author's contribution towards the manuscript have been illustrated below:

Professor Shuangfei Li, as the first author, collected, processed and analyzed the data. He was also responsible for all drafts of the manuscript.

Professor Xuewei Yang, as the corresponding author, was responsible for the conceptualization of the study, design and planning of the manuscript, as well as the analysis and interpretation of the results.

Dr. Liangxu Liu, as the coauthor, was responsible for analyzing the data and improving the figure quality, English writing and discussion section of the manuscript.

Professor Jay Jiayang Cheng, as the coauthor, was responsible for critical reading and finalization of the manuscript.

Funding information This project was partially supported by the development special funds of Shenzhen Strategic Emerging Industries and Future Industries (Grant No. KJYY20180201180253571), Shenzhen Science and Technology Innovation Shenzhen-Hong Kong Joint Research Project (Grant No. SGLH20180622152010394), and Shenzhen Overseas High-level Talent Innovation and Entrepreneurship Special Fund Project (Grant No. KQJSCX20180328093806045).

Compliance with ethical standards

Conflict of interest The authors declare that they have no conflict of interest.

Statement of informed consent Not applicable.

References

1. Field CB, Campbell JE, Lobell DB (2008) Biomass energy: the scale of the potential resource. Trends Ecol Evol 23(2):65–72
2. Chisti Y (2007) Biodiesel from microalgae. Biotechnol Adv 25(3): 294–306
3. Clarens AF, Resurreccion EP, White MA, Colosi LM (2010) Environmental life cycle comparison of algae to other bioenergy feedstocks. Environmental Science & Technology 44(5):1813–1819
4. Callegari A, Bolognesi S, Cecconet D, Capodaglio AG (2019) Production technologies, current role, and future prospects of biofuels feedstocks: a state-of-the-art review. Crit Rev Environ Sci Technol:1–53
5. Mohan D, Pittman CU, Steele PH (2006) Pyrolysis of wood/biomass for bio-oil: a critical review. Energy Fuel 20(3):848–889
6. Kara B, Emir Z, Kaygusuz K (2012) Thermal processing technologies for biomass conversion to energy. Journal of Engineering Research and Applied Science 1(1):55–62
7. Yang X, Zhang R, Fu J, Geng S, Cheng JJ, Sun Y (2014) Pyrolysis kinetic and product analysis of different microalgal biomass by distributed activation energy model and pyrolysis–gas chromatography–mass spectrometry. Bioresour Technol 163:335–342
8. Chen W-H, Chu Y-S, Liu J-L, Chang J-S (2018) Thermal degradation of carbohydrates, proteins and lipids in microalgae analyzed by evolutionary computation. Energy Convers Manag 160:209–219
9. Ghosh A, Khanra S, Mondal M, Halder G, Tiwari O, Saini S, Bhowmick TK, Gayen K (2016) Progress toward isolation of strains and genetically engineered strains of microalgae for production of biofuel and other value added chemicals: a review. Energy Convers Manag 113:104–118
10. Pielichowski K, Njuguna J (2005) Thermal degradation of polymeric materials. Smithers Rapra Technology,
11. Marcilla A, Gómez-Siurana A, Gomis C, Chápuli E, Catalá MC, Valdés FJ (2009) Characterization of microalgal species through TGA/FTIR analysis: application to< i> nannochloropsis</i> sp. Thermochim Acta 484(1):41–47
12. Allen MM (1968) Simple conditions for growth of unicellular blue-green algae on plates1, 2. J Phycol 4(1):1–4
13. Williams S (1984) Official methods of analysis of the Association of Official Analytical Chemists vol Ed 14
14. Aguilera-Morales M, Casas-Valdez M, Carrillo-Domınguez S, González-Acosta B, Pérez-Gil F (2005) Chemical composition and microbiological assays of marine algae< i> Enteromorpha</i> spp. as a potential food source. J Food Compos Anal 18(1): 79–88
15. Franklin ST, Martin KR, Baer RJ, Schingoethe DJ, Hippen AR (1999) Dietary marine algae (Schizochytrium sp.) increases

concentrations of conjugated linoleic, docosahexaenoic and transvaccenic acids in milk of dairy cows. J Nutr 129(11):2048–2054
16. Vardon DR, Sharma B, Scott J, Yu G, Wang Z, Schideman L, Zhang Y, Strathmann TJ (2011) Chemical properties of biocrude oil from the hydrothermal liquefaction of< i> Spirulina</i> algae, swine manure, and digested anaerobic sludge. Bioresour Technol 102(17):8295–8303
17. Rebolloso Fuentes M, Acién Fernández G, Sánchez Pérez J, Guil Guerrero J (2000) Biomass nutrient profiles of the microalga< i> Porphyridium cruentum</i>. Food Chem 70(3):345–353
18. Pv VS, Robertson J, Lewis B (1991) Methods for dietary fiber, neutral detergent fiber, and nonstarch polysaccharides in relation to animal nutrition. J Dairy Sci 74(10):3583–3597
19. Cochran R, Adams D, Wallace J, Galyean M (1986) Predicting digestibility of different diets with internal markers: evaluation of four potential markers. J Anim Sci 63(5):1476–1483
20. Hatfield RD, Jung HJG, Ralph J, Buxton DR, Weimer PJ (1994) A comparison of the insoluble residues produced by the Klason lignin and acid detergent lignin procedures. J Sci Food Agric 65(1):51–58
21. Dien BS, Jung HJG, Vogel KP, Casler MD, Lamb JAFS, Iten L, Mitchell RB, Sarath G (2006) Chemical composition and response to dilute-acid pretreatment and enzymatic saccharification of alfalfa, reed canarygrass, and switchgrass. Biomass Bioenergy 30(10): 880–891
22. Zhou D, Zhang L, Zhang S, Fu H, Chen J (2010) Hydrothermal liquefaction of macroalgae Enteromorpha prolifera to bio-oil. Energy Fuel 24(7):4054–4061
23. Almeida JR, Modig T, Petersson A, Hähn-Hägerdal B, Lidén G, Gorwa-Grauslund MF (2007) Increased tolerance and conversion of inhibitors in lignocellulosic hydrolysates by Saccharomyces cerevisiae. J Chem Technol Biotechnol 82(4):340–349
24. Okuda K, Oka K, Onda A, Kajiyoshi K, Hiraoka M, Yanagisawa K (2008) Hydrothermal fractional pretreatment of sea algae and its enhanced enzymatic hydrolysis. J Chem Technol Biotechnol 83(6):836–841
25. Martone PT, Estevez JM, Lu F, Ruel K, Denny MW, Somerville C, Ralph J (2009) Discovery of lignin in seaweed reveals convergent evolution of cell-wall architecture. Curr Biol 19(2):169–175
26. Delwiche CF, Graham LE, Thomson N (1989) Lignin-like compounds and sporopollenin in coleochaete, an algal model for land plant ancestry. Science 245(4916):399–401
27. Moon RJ, Martini A, Nairn J, Simonsen J, Youngblood J (2011) Cellulose nanomaterials review: structure, properties and nanocomposites. Chem Soc Rev 40(7):3941–3994
28. Yang X, Zeng Y, Ma F, Zhang X, Yu H (2010) Effect of biopretreatment on thermogravimetric and chemical characteristics of corn stover by different white-rot fungi. Bioresour Technol 101(14):5475–5479
29. Shen D, Gu S, Bridgwater AV (2010) Study on the pyrolytic behaviour of xylan-based hemicellulose using TG–FTIR and Py–GC–FTIR. J Anal Appl Pyrolysis 87(2):199–206
30. Chen G, Leung D (2003) Experimental investigation of biomass waste, (rice straw, cotton stalk, and pine sawdust), pyrolysis characteristics. Energy Sources 25(4):331–337
31. Grønli MG, Várhegyi G, Di Blasi C (2002) Thermogravimetric analysis and devolatilization kinetics of wood. Ind Eng Chem Res 41(17):4201–4208
32. Sugiyama J, Vuong R, Chanzy H (1991) Electron diffraction study on the two crystalline phases occurring in native cellulose from an algal cell wall. Macromolecules 24(14):4168–4175
33. Yang H, Yan R, Chen H, Lee DH, Zheng C (2007) Characteristics of hemicellulose, cellulose and lignin pyrolysis. Fuel 86(12–13): 1781–1788
34. Sonobe T, Worasuwannarak N (2008) Kinetic analyses of biomass pyrolysis using the distributed activation energy model. Fuel 87(3): 414–421
35. Balooch M, Cardillo M, Miller D, Stickney R (1974) Molecular beam study of the apparent activation barrier associated with adsorption and desorption of hydrogen on copper. Surf Sci 46(2):358–392
36. Marsanich K, Barontini F, Cozzani V, Petarca L (2002) Advanced pulse calibration techniques for the quantitative analysis of TG–FTIR data. Thermochim Acta 390(1):153–168
37. Biagini E, Barontini F, Tognotti L (2006) Devolatilization of biomass fuels and biomass components studied by TG/FTIR technique. Ind Eng Chem Res 45(13):4486–4493
38. Lv G, Wu S, Lou R, Yang Q (2010) Analytical pyrolysis characteristics of enzymatic/mild acidolysis lignin from sugarcane bagasse. Cellulose Chemistry & Technology 44(9):335
39. Peng Y, Wu S (2011) Fast pyrolysis characteristics of sugarcane bagasse hemicellulose. Cellul Chem Technol 45(9):605